

# They are Not Completely Useless: Towards Recycling Transferable Unlabeled Data for Class-Mismatched Semi-Supervised Learning

Zhuo Huang<sup>1</sup> Ying Tai<sup>2</sup> Chengjie Wang<sup>2</sup> Jian Yang<sup>1,3</sup> Chen Gong<sup>1,4</sup>

<sup>1</sup>School of Computer Science and Engineering, Nanjing University of Science and Technology

<sup>2</sup>YouTu Lab, Tencent

<sup>3</sup>Jiangsu Key Lab of Image and Video Understanding for Social Security

<sup>4</sup>The Department of Computing, HongKong Polytechnic University

{hzhuo, csjyang, chen.gong}@njust.edu.cn; {yingtai, jasoncjwang}@tencent.com

## Abstract

*Semi-Supervised Learning (SSL) with mismatched classes deals with the problem that the classes-of-interests in the limited labeled data is only a subset of the classes in massive unlabeled data. As a result, the classes only possessed by the unlabeled data may mislead the classifier training and thus hindering the realistic landing of various SSL methods. To solve this problem, existing methods usually divide unlabeled data to in-distribution (ID) data and out-of-distribution (OOD) data, and directly discard or weaken the OOD data to avoid their adverse impact. In other words, they treat OOD data as completely useless and thus the potential valuable information for classification contained by them is totally ignored. To remedy this defect, this paper proposes a “Transferable OOD data Recycling” (TOOR) method which properly utilizes ID data as well as the “recyclable” OOD data to enrich the information for conducting class-mismatched SSL. Specifically, TOOR firstly attributes all unlabeled data to ID data or OOD data, among which the ID data are directly used for training. Then we treat the OOD data that have a close relationship with ID data and labeled data as recyclable, and employ adversarial domain adaptation to project them to the space of ID data and labeled data. In other words, the recyclability of an OOD datum is evaluated by its transferability, and the recyclable OOD data are transferred so that they are compatible with the distribution of known classes-of-interests. Consequently, our TOOR method extracts more information from unlabeled data than existing approaches, so it can achieve the improved performance which is demonstrated by the experiments on typical benchmark datasets.*

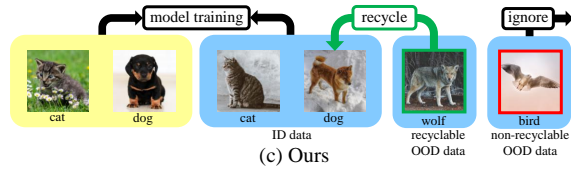
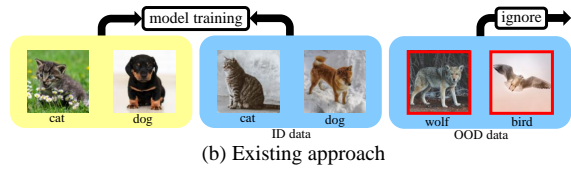
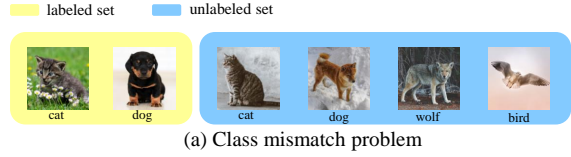


Figure 1. Motivation of our work. (a) Illustration of class mismatch problem. (b) Strategy of existing approaches which utilizes ID data, and meanwhile discarding all the OOD data. (c) Main idea of our method which utilizes the ID data as well as the recyclable OOD data, and then ignore the non-recyclable OOD data.

## 1. Introduction

The shortage of labeled data has become a noticeable bottleneck for training many traditional machine learning or computer vision models, as manually annotating a large number of data is usually prohibitive due to the unaffordable monetary cost or huge demand in human resource. Therefore, a popular solution for dealing with such problem is Semi-Supervised Learning (SSL) [7], which has been proven to be effective in harnessing scarce labeled data and abundant unlabeled data for training an accurate classifier.

Conventional SSL includes graph-based methods [14, 36, 45] which exploit unlabeled data on a constructed graph

through label propagation, semi-supervised support vector machines [2] which utilizes the max-margin theory to learn the decision boundary with the help of unlabeled data, and co-training [4] which integrates the label decisions of two peered learners on unlabeled data. Recently, the research on SSL has made significant progress based on deep neural networks [23] with strong representation ability, and they usually utilize three types of training strategy to handle both labeled and unlabeled data, namely: 1) *consistency regularization* [19, 22, 26, 28, 34, 44] which enforces that the perturbations on unlabeled data should not change their label predictions significantly; 2) *entropy minimization* [16, 24] which impels networks to make confident predictions on unlabeled data; and 3) *data augmentation* [3, 33, 37, 42] which creates additional examples as well as label information to improve the generalizability of the learned classifier.

However, the above-mentioned SSL approaches rely on a basic assumption that the classes contained by labeled data (*i.e.*,  $\mathcal{C}_l$ ) and those contained by unlabeled data (*i.e.*,  $\mathcal{C}_u$ ) are the same, namely  $\mathcal{C}_l = \mathcal{C}_u$ . Unfortunately, in real-world situations, such assumption is difficult to satisfy as we actually do not know the labels of unlabeled data in advance. Such problem for realistic SSL is called *class mismatch* [30] if some of the classes in unlabeled data are different from those in labeled examples, as shown in Figure 1(a). Concretely, class mismatch means that the classes in labeled data  $\mathcal{C}_l$  constitute a subset of the classes in unlabeled data  $\mathcal{C}_u$ , namely  $\mathcal{C}_l \subseteq \mathcal{C}_u$  and  $\mathcal{C}_l \cup \mathcal{C}_u = \mathcal{C}_u$ . Here the unlabeled data that belong to the classes  $\mathcal{C}_l$  are called *in-distribution* (ID) data, while the unlabeled data only belonging to  $\mathcal{C}_u$  are called *out-of-distribution* (OOD) data. Due to the existence of OOD data, the traditional SSL methods will be confused and thus generating the degraded test performance regarding the interested classes  $\mathcal{C}_l$ .

To solve the class mismatch problem, current works focus on leveraging ID data while trying to eliminate the negative impact caused by the OOD data. For example, Chen *et al.* [9] propose a self-distillation method to filter out the probable OOD data based on their confidence scores. Guo *et al.* [17] utilize a weighting mechanism to decrease the influence of OOD data as well as emphasize the ID data in unlabeled set. As shown in Figure 1 (b), both methods regard OOD data as completely harmful which should be discarded or weakened. However, here we argue that not all the OOD data are useless, and some of them are informative and can actually be re-used in a suitable way to improve the classification performance. Considering an example, if “dog” and “cat” are two classes of our interests in  $\mathcal{C}_l$  to be classified, and the examples of “wolf” and “car” are private in  $\mathcal{C}_u$  forming the OOD data. In this case, the unlabeled examples with potential label “wolf” is much more useful than those of “car” in classifying “dog” and “cat” in  $\mathcal{C}_l$ , as wolf and dog image examples can be very similar in feature space.

As a sequel, they can be activated for our classification task even though they are OOD data. In other words, the prior works [9, 17] tackling class-mismatch problem only deploy the ID data in unlabeled set, while our method employs both ID data and some useful task-oriented OOD data to train an improved semi-supervised classifier, which is shown in Figure 1 (c). This is similar to the garbage recycling in our daily life, where the useful part in garbage can be recycled to create extra economic value. Here although the OOD data seem to be useless at the first glance, some of them are still beneficial for SSL training if they are properly used.

Based on the above considerations, in this paper, we propose a “Transferable OOD Data Recycling” (TOOR) method for semi-supervised learning under class mismatch which exploits the ID data and simultaneously recycles transferable OOD data in unlabeled set for training a SSL model. Specifically, TOOR divides the entire unlabeled set into three subsets in each training round, namely ID data, recyclable OOD data, and non-recyclable OOD data, where only the last subset is discarded for network training. Here ID data are automatically detected according to the fact that the softmax score of ID data would be higher than that of OOD data, while recyclable OOD data and non-recyclable OOD data are decided by evaluating the transferability from them to the feature space of the labeled image examples. For recyclable OOD data, as their distribution still slightly differs from the labeled data, we propose to conduct domain adaptation through adversarial learning [5, 6, 8, 10, 12, 31, 35, 39, 43] to reduce the potential gap between the two feature distributions. Hence, TOOR is able to learn on more examples than [9, 17] since the transferable OOD data are also well adapted to the space of the labeled data to aid SSL training. Thanks to the re-use of transferable OOD data, our TOOR method can be incorporated by many existing SSL approaches (*e.g.*, Mean Teacher [34],  $\Pi$  model [22] and VAT [28]) so that the class mismatch can be effectively tackled. Comprehensive experiments on CIFAR-10 and SVHN datasets reveal that TOOR consistently outperforms other baselines under different numbers of mismatched OOD data in unlabeled set.

## 2. The Proposed TOOR Approach

This section presents our proposed TOOR approach. In our class-mismatched SSL setting, we use the notations  $\mathcal{X}$  and  $\mathcal{Y}$  to denote the feature space and label space, respectively. Given a set of training examples  $\mathcal{D} = \{\mathbf{x}_i \in \mathcal{X} \subset \mathbb{R}^d, i = 1, 2, \dots, n, n = l + u \text{ with } l \ll u\}$  in which the first  $l$  examples are labeled with  $\{y_i\}_{i=1}^l \in \mathcal{Y} \in \{1, 2, \dots, c\}$  where  $c$  is the number of known classes, and the remaining  $u$  examples are unlabeled. We use  $\mathcal{D}_l = \{(\mathbf{x}_1, y_1), (\mathbf{x}_2, y_2), \dots, (\mathbf{x}_l, y_l)\}$  to denote the labeled set drawn from the joint distribution  $P$  defined on  $\mathcal{X} \times \mathcal{Y}$ , and  $\mathcal{D}_u = \{\mathbf{x}_{l+1}, \mathbf{x}_{l+2}, \dots, \mathbf{x}_{l+u}\}$  to represent the unlabeled

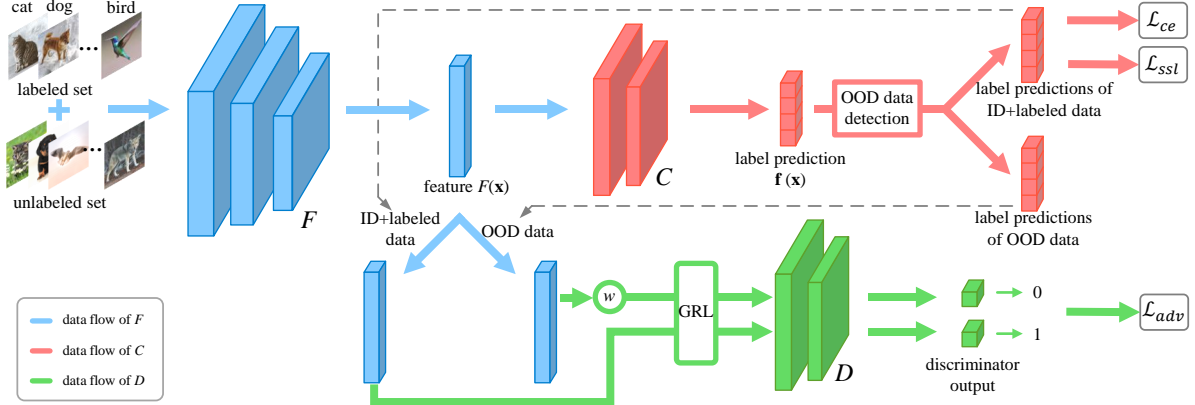


Figure 2. The pipeline of our Transferable OOD data Recycling (TOOR) method, in which  $F$ ,  $C$  and  $D$  denote the feature extractor, classifier, and discriminator, respectively. Given the labeled set and unlabeled set,  $F$  extracts the feature  $F(\mathbf{x})$  for each input image, which is then sent to  $C$  to obtain the label prediction vector  $\mathbf{f}(\mathbf{x})$  which encodes the probabilities of  $\mathbf{x}$  to different classes. Based on  $\mathbf{f}(\mathbf{x})$ , the OOD data detection module decides whether  $\mathbf{x}$  is an ID datum or an OOD datum. Then the determined ID data are used to compute  $\mathcal{L}_{ce}$  and  $\mathcal{L}_{ssl}$ , and the determined OOD data are further decided to be recyclable or not. Based on the result of OOD data detection, we obtain the features of ID data and OOD data separately (see the gray dashed lines). Finally, the OOD data are weighted by the transferability score  $w(\mathbf{x})$ , and some of them are recycled by the adversarial learning process composed of the generator  $F$  and discriminator  $D$ . ‘‘GRL’’ denotes the gradient reversal layer [11] that accomplishes adversarial learning. The above procedure including OOD data detection and adversarial learning for data recycling iterates until all ID data are found and transferable OOD data are recycled.

set. Particularly,  $\mathcal{D}_u$  is assumed to be composed of an ID dataset  $\mathcal{D}_{id}$  whose labels are in  $\mathcal{Y}$  and an OOD dataset  $\mathcal{D}_{ood}$  whose labels are in  $\mathcal{Y}'$  with typically  $\mathcal{Y} \subset \mathcal{Y}'$ , *i.e.*,  $\mathcal{D}_u = \mathcal{D}_{id} \cup \mathcal{D}_{ood}$ .

The main goal of TOOR is to effectively utilize the class mismatched training set  $\mathcal{D} = \mathcal{D}_l \cup \mathcal{D}_u$  to find a semi-supervised classifier that can properly leverage  $\mathcal{D}_u$  so that any unseen image  $\mathbf{x}$  with unknown true label  $y \in \mathcal{Y}$  can be correctly classified. The model of TOOR can be concisely formulated by the following optimization problem:

$$\begin{aligned}
 & \min_{\theta_F, \theta_C} \max_{\theta_D} \underbrace{\frac{1}{l} \sum_{i=1}^l \mathcal{L}_{ce}(C(F(\mathbf{x}_i)), y_i)}_{\text{supervised fidelity term}} \\
 & + \lambda \underbrace{\frac{1}{l + |\mathcal{D}_{id}|} \sum_{\mathbf{x}_i \in \mathcal{D}_{id} \cup \mathcal{D}_l} \mathcal{L}_{ssl}(\mathbf{x}_i; \theta_F, \theta_C)}_{\text{ID data exploration term}} \\
 & + \gamma \underbrace{\frac{1}{|\mathcal{D}_{ood}|} \sum_{\mathbf{x}_i \in \mathcal{D}_{ood}} w(\mathbf{x}_i) \cdot \mathcal{L}_{adv}(\mathbf{x}_i; \theta_F, \theta_D)}_{\text{OOD data recycling term}}
 \end{aligned} \quad (1)$$

in which  $F$  is an image feature extractor,  $C$  is a classifier,  $D$  is a discriminator, and  $\theta_F$ ,  $\theta_C$  and  $\theta_D$  are their parameters, respectively. The notation ‘‘ $|\cdot|$ ’’ denotes the size of the corresponding set. In Eq. (1), the first term is dubbed *supervised fidelity term* which involves the standard cross-entropy loss  $\mathcal{L}_{ce}(\cdot)$  to compare the network prediction  $C(F(\mathbf{x}_i))$  on ev-

ery labeled image and its ground-truth label  $y_i$ . The second term refers to *ID data exploration term* in which  $\mathcal{L}_{ssl}(\cdot)$  denotes the loss defined on ID data and it can be any regularizer in existing SSL method such as consistency regularizer [22, 34] or manifold regularizer [1, 13, 40]. The third term is termed *OOD data recycling term* which introduces an adversarial learning loss  $\mathcal{L}_{adv}(\cdot)$  to ‘‘recycle’’ the transferable OOD data. Here the OOD data are found by examining their transferability score  $w(\mathbf{x}_i)$  which will be detailed in Section 2.2. Through such recycling procedure, our TOOR approach can maximally exploit class-mismatched dataset without including useless or harmful OOD data, and meanwhile re-use the rich information contained by the transferable unlabeled image examples, leading to superior performance to other methods. The parameters  $\lambda$  and  $\gamma$  are nonnegative coefficients that control the relative weights of the above three terms.

The general procedure of the proposed TOOR algorithm is shown in Figure 2. Given the labeled image set  $\mathcal{D}_l$  and unlabeled image set  $\mathcal{D}_u$ , we use the feature extractor  $F$  to compute the feature representations  $F(\mathbf{x})$  for  $\mathbf{x} \in \mathcal{D}_l \cup \mathcal{D}_u$ . Then, a classifier  $C$  is imposed on  $F(\mathbf{x})$  to obtain the label prediction vector  $\mathbf{f}(\mathbf{x})$  for each of the input images. Based on  $\mathbf{f}(\mathbf{x})$ , the ID data can be found which are used to compute  $\mathcal{L}_{ssl}$  together with the labeled data. The decided OOD data are further sent to the adversarial learning branch so that the recyclable OOD data are called back and the non-recyclable OOD data are completely discarded. Specifically, all OOD data weighted with the transferability

score  $w(\mathbf{x})$  are combined with the ID data to act as a generator, and they are employed to confuse the discriminator  $D$ . Then  $D$  should try its best to distinguish the presented data as ID data (*i.e.*, 1) or OOD data (*i.e.*, 0). During the iterative process between OOD data detection and adversarial learning for recycling, our detected ID dataset expands from the initial limited labeled image set by gradually absorbing the considered ID images and the transferable OOD images. From the above explanations on the procedure of our TOOR, we see that OOD data detection, adversarial learning for recycling, and semi-supervised learning parts are critical in our method, and they will be detailed in Sections 2.1, 2.2, and 2.3, respectively.

## 2.1. OOD Data Detection

*OOD data detection* aims to correctly distinguish the unlabeled image data into ID data and OOD data. Many existing works [18, 25] have shown that it can be accomplished by investigating the softmax scores of unlabeled data during network training. Specifically, given an input image  $\mathbf{x}$ , its label prediction  $\mathbf{f}(\mathbf{x})$  output by the classifier is a  $c$ -dimensional vector  $[f_1(\mathbf{x}), f_2(\mathbf{x}), \dots, f_c(\mathbf{x})]^\top$ , where  $\{f_i(\mathbf{x})\}_{i=1}^c$  can be interpreted as the probability that  $\mathbf{x}$  belongs to class  $i$ . Therefore, the class response of  $\mathbf{x}$  on the  $i$ -th class can be computed as

$$S_i(\mathbf{x}; T) = \frac{\exp(f_i(\mathbf{x})/T)}{\sum_{j=1}^c \exp(f_j(\mathbf{x})/T)}, \quad (2)$$

where  $T \in \mathbb{R}^+$  is a temperature scaling [18, 25] parameter and is usually set to 1 during training. Here the maximum softmax probability among  $S_i(\mathbf{x}; T)$  across  $i = \{1, \dots, c\}$  is dubbed *softmax score* [25], which is computed as

$$S(\mathbf{x}; T) = \max_{i \in \{1, \dots, c\}} S_i(\mathbf{x}; T). \quad (3)$$

It has been demonstrated in [25] that the softmax scores of ID data are significantly larger than those of OOD data, and thus the softmax scores of different examples can be utilized to judge the unlabeled images as ID data or OOD data.

However, in our TOOR approach, due to the aforementioned gradual expansion of ID dataset during the training process, the softmax scores of certain OOD data may oscillate, which make their results of OOD data detection not consistent across successive iterations. To address this problem, we conduct temporal ensembling [22] to yield stabilized scores on all unlabeled data. Concretely, we assemble the softmax scores of unlabeled data from historical iterations via using exponential moving average (EMA), which assigns greater weights to recent softmax scores while exponentially decreasing the weights of early softmax scores. Therefore, the assembled score of  $\mathbf{x}$  is computed as

$$\hat{S}(\mathbf{x}; T)^{(t)} = \eta \hat{S}(\mathbf{x}; T)^{(t-1)} + (1 - \eta) S(\mathbf{x}; T)^{(t)}, \quad (4)$$

where  $S(\mathbf{x}; T)^{(t)}$  denotes the softmax score computed according to Eq. (3) at the  $t$ -th iteration,  $\hat{S}(\mathbf{x}; T)^{(t)}$  and  $\hat{S}(\mathbf{x}; T)^{(t-1)}$  denote the assembled softmax score at the  $t$ -th iteration and the  $(t-1)$ -th iteration, respectively. The coefficient  $\eta \in [0, 1]$  is a momentum term that decides how far the ensemble reaches into training history. Such assembled score varies smoothly and will not be significantly changed across different iterations, enabling our method to make stable identification on OOD data.

Given the assembled score computed in Eq. (4), we use a threshold  $\delta$  to separate OOD data from ID data in the unlabeled set  $\mathcal{D}_u$ . Specifically, an image is considered as an ID datum if its assembled score is larger than  $\delta$ , and an OOD datum otherwise. By introducing  $t(\mathbf{x}; \delta)$  as an indication variable regarding  $\mathbf{x}$ , this process is formulated as

$$t(\mathbf{x}; \delta) = \begin{cases} 1, & \text{if } \hat{S}(\mathbf{x}; T) > \delta \\ 0, & \text{if } \hat{S}(\mathbf{x}; T) \leq \delta \end{cases}. \quad (5)$$

That is to say, the images  $\mathbf{x}$ 's with  $t(\mathbf{x}; \delta) = 1$  are determined as ID data and they will be incorporated by  $\mathcal{D}_{id}$  to compute the ID data exploration term in Eq. (1). The experimental results in Section 3.3 show that the assembled score can lead to impressive performance.

## 2.2. Adversarial Learning for Recycling

After detecting the OOD data as mentioned in the above subsection, now we should find the recyclable images in  $\mathcal{D}_{ood}$  and then transfer them to the space of  $\mathcal{D}_l \cup \mathcal{D}_{id}$  such that their contained information can be fully extracted for training a semi-supervised classifier. To this end, we treat  $\mathcal{D}_{ood}$  as source domain and  $\mathcal{D}_l \cup \mathcal{D}_{id}$  as target domain, and propose to use adversarial domain adaptation to achieve this goal. Adversarial domain adaptation [5, 6, 12, 35, 43] aims to learn class discriminative and domain invariant features by using adversarial learning [15]. In our case, the parameters  $\theta_D$  of the discriminator  $D$  are learned to distinguish the previous identified OOD data and ID data by minimizing a cross-entropy loss. Meanwhile, the parameters  $\theta_F$  of the feature extractor  $F$  are trained to deceive the discriminator by maximizing the same cross-entropy loss. In this way, the domain shift between ID data and transferable OOD data is closed in which the OOD data that are “easily” transferred are likely to be recycled. The above adversarial process can be formulated as the min-max game below:

$$\begin{aligned} \min_{\theta_F} \max_{\theta_D} \mathcal{L}_{adv} = & \frac{1}{|\mathcal{D}_{ood}|} \sum_{\mathbf{x}_i \in \mathcal{D}_{ood}} w(\mathbf{x}_i) \log D(F(\mathbf{x}_i)) \\ & + \frac{1}{|\mathcal{D}_{id}| + l} \sum_{\mathbf{x}_i \in \mathcal{D}_{id} \cup \mathcal{D}_l} \log(1 - D(F(\mathbf{x}_i))), \end{aligned} \quad (6)$$

where  $w(\mathbf{x}_i)$  is the transferability score that helps to find recyclable OOD data, and the computation of this score

will be detailed later. Through such a min-max optimization procedure, the two adversarial opponents converge to a situation where the features of transferable OOD data will be pushed near to the labeled data and ID data, so as to fool the discriminator. Note that we also train the classifier  $C$  by minimizing the supervised cross-entropy loss  $\mathcal{L}_{ce}$  on the original labeled data, which is simultaneously conducted with adversarial learning. Hence, we can successfully extract the helpful knowledge from OOD data for our classification task on the interested label space  $\mathcal{Y}$ .

Here we propose to utilize two cues to find the potential transferable OOD data from the unlabeled set  $\mathcal{D}_u$ . Firstly, if the discriminator  $D$  cannot tell whether an image  $\mathbf{x}_i \in \mathcal{D}_u$  is from the source domain or the target domain, we know that  $\mathbf{x}_i$  is quite ambiguous as its representation is close to both ID data and OOD data. Therefore, it is likely to be a transferable image example that should be recycled. To depict this, we introduce a *domain similarity score*  $w_d(\mathbf{x}_i)$  for  $\mathbf{x}_i$ . Secondly, if the classifier  $C$  attributes  $\mathbf{x}_i$  to a certain class  $y \in \mathcal{Y}$  with a strong tendency, we learn that  $\mathbf{x}_i$  probably belongs to this class. To describe this, we introduce a *class tendency score*  $w_c(\mathbf{x}_i)$ . By adaptively integrating  $w_d(\mathbf{x}_i)$  and  $w_c(\mathbf{x}_i)$ , we acquire the transferability score  $w(\mathbf{x}_i)$  for any  $\mathbf{x}_i \in \mathcal{D}_u$ , which serves as the weight for  $\mathbf{x}_i$  to perform the min-max game in Eq. (6). In the following, we explain the computations for  $w_d(\mathbf{x}_i)$ ,  $w_c(\mathbf{x}_i)$  and the integrated  $w(\mathbf{x}_i)$ .

**Domain similarity score**  $w_d(\mathbf{x}_i)$ . Our discriminator  $D$  is trained to distinguish ID data from OOD data. The output of discriminator can be interpreted as

$$D(F(\mathbf{x}_i)) = p(\mathbf{x}_i \in \mathcal{D}_{id} \mid \mathbf{x}_i), \mathbf{x}_i \in \mathcal{D}_u, \quad (7)$$

where  $p(\cdot)$  denotes probability in this paper. Eq. (7) means that the output value of domain discriminator provides the likelihood of an OOD example  $\mathbf{x}_i$  belonging to the domain of  $\mathcal{D}_{id}$ . Consequently, if  $D(F(\mathbf{x}_i))$  is large, we know that  $\mathbf{x}_i$  is similar to the known space of  $\mathcal{D}_l \cup \mathcal{D}_{id}$ . As a result, we should properly recycle these examples by assigning them large scores. On the other hand, if  $D(F(\mathbf{x}_i))$  is small, the corresponding  $\mathbf{x}_i$  might not come from the space of  $\mathcal{D}_l \cup \mathcal{D}_{id}$ . These images should have small scores such that both the discriminator and the classifier will ignore them. Hence, the score reflecting domain information is formulated as

$$\tilde{w}_d(\mathbf{x}_i) = D(F(\mathbf{x}_i)). \quad (8)$$

To obtain more discriminative score assignments across OOD data, we follow [6, 43] and normalize the scores of all  $\mathbf{x}_i \in \mathcal{D}_{ood}$  to compute domain similarity score, which is

$$w_d(\mathbf{x}_i) = \frac{\tilde{w}_d(\mathbf{x}_i)}{\frac{1}{B} \sum_{j=1}^B \tilde{w}_d(\mathbf{x}_j)}, \mathbf{x}_i \in \mathcal{D}_{ood}, \quad (9)$$

where  $B$  is the mini-batch size set to 100 as in [6, 43]. The normalization equipped with the mini-batch-aided normal-

izer helps enlarging the scores for the potential recyclable OOD data, and meanwhile decreasing the scores of non-transferable OOD data to prevent them from being recycled.

**Class tendency score**  $w_c(\mathbf{x}_i)$ . Apart from the domain similarity score, the label predictions of OOD data generated by  $C$  also contain rich transferability information. Concretely, the label predictions of ID data can provide valuable clue in evaluating the transferability since the classifier  $C$  has been trained on labeled set  $\mathcal{D}_l$  and thus possessing considerable discriminability. Hence, inspired by [38], we employ the predictive margin between the largest and the second-largest elements of label prediction vector  $\mathbf{f}(\mathbf{x}_i)$  to establish class tendency score, which is computed as

$$\tilde{w}_c(\mathbf{x}_i) = \max_{j \in \{1, \dots, c\}} f_j(\mathbf{x}_i) - \max_{k \in \{1, \dots, c\}, k \neq j} f_k(\mathbf{x}_i). \quad (10)$$

If the predictive margin of an OOD example is large, it implies that the example has relatively large tendency to one certain category, then we consider such OOD examples as transferable data and they could be recycled to the corresponding class  $j$ . On the other hand, if the margin is small, which means that the label of this example is quite unclear, it should be excluded for recycling. Similar to the operation on domain similarity score  $w_d(\mathbf{x}_i)$ , here we also normalize  $w_c(\mathbf{x}_i)$  as Eq. (9), which is formulated as

$$w_c(\mathbf{x}_i) = \frac{\tilde{w}_c(\mathbf{x}_i)}{\frac{1}{B} \sum_{j=1}^B \tilde{w}_c(\mathbf{x}_j)}, \mathbf{x}_i \in \mathcal{D}_{ood}. \quad (11)$$

**Adaptive integration of  $w_d(\mathbf{x}_i)$  and  $w_c(\mathbf{x}_i)$ .** To calculate the transferability scores of all OOD data, we need to combine the obtained domain similarity scores and class tendency scores in a proper way. Specifically, these two scores should be explicitly weighted to yield good performance. By employing the vectors  $\mathbf{w}_d = [w_d(\mathbf{x}_1), \dots, w_d(\mathbf{x}_{|\mathcal{D}_{ood}|})]^\top$  and  $\mathbf{w}_c = [w_c(\mathbf{x}_1), \dots, w_c(\mathbf{x}_{|\mathcal{D}_{ood}|})]^\top$  to encode the domain similarity scores and class tendency scores for all  $\mathbf{x}_i \in \mathcal{D}_{ood}$ , here we propose to utilize their variances to compute the trade-off weights. Concretely, if the variance of  $w_d(\mathbf{x}_i)$  or  $w_c(\mathbf{x}_i)$  is large, which means that the values of contained elements are discriminative for characterizing the transferability of all  $\mathbf{x}_i \in \mathcal{D}_{ood}$ , then it should be paid more attention in composing the final transferability score  $w(\mathbf{x}_i)$ . In contrast, if the variance of  $w_d(\mathbf{x}_i)$  or  $w_c(\mathbf{x}_i)$  is small, then it is less helpful in evaluating the transferability of  $\mathbf{x}_i$ , so its contribution in computing  $w(\mathbf{x}_i)$  should be suppressed. Mathematically, we have the following convex combination:

$$w(\mathbf{x}_i) = \frac{\text{var}(\mathbf{w}_d)}{\text{var}(\mathbf{w}_d) + \text{var}(\mathbf{w}_c)} w_d(\mathbf{x}_i) + \frac{\text{var}(\mathbf{w}_c)}{\text{var}(\mathbf{w}_d) + \text{var}(\mathbf{w}_c)} w_c(\mathbf{x}_i), \quad (12)$$

<b>Algorithm 1</b> The training process for our TOOR method	
<b>Input:</b>	Labeled set $\mathcal{D}_l = \{(\mathbf{x}_1, y_1), \dots, (\mathbf{x}_l, y_l)\}$ , class-mismatched unlabeled set $\mathcal{D}_u = \{\mathbf{x}_{l+1}, \dots, \mathbf{x}_{l+u}\}$ .
1:	Train feature extractor $F$ and classifier $C$ on labeled set $\mathcal{D}_l$ by minimizing the supervised fidelity term in Eq. (1);
2:	<b>for</b> $i = 1$ to MaxIter <b>do</b>
3:	Compute softmax score $S(\mathbf{x}; T)$ according to Eq. (3) and the assembled softmax score $\hat{S}(\mathbf{x}; T)$ according to Eq. (4);
4:	Perform OOD data detection to find the ID dataset $\mathcal{D}_{id}$ and OOD dataset $\mathcal{D}_{ood}$ through Eq. (5);
5:	Weigh each OOD datum $\mathbf{x}$ with the transferability score $w(\mathbf{x})$ by Eq. (12);
6:	OOD data recycling and network training by minimizing Eq. (1).
7:	<b>end for</b>
<b>Output:</b>	Discriminator parameter $\theta_D$ ; and SSL model with parameters $\theta_F$ and $\theta_C$ for classification.

where  $\text{var}(\cdot)$  denotes the variance computation regarding the input vector. Since we have re-scaled the range of these two scores  $w_d(\mathbf{x}_i)$  and  $w_c(\mathbf{x}_i)$  to the same level as in Eqs. (9) and (11), the variances of them can be directly employed to compare their importance in composing the transferability score  $w(\mathbf{x}_i)$ . Finally, we can find the transferable OOD data by weighing each OOD datum with  $w(\mathbf{x}_i)$  and then perform the weighted min-max game as Eq. (6).

After the transferable OOD data have been recycled by the above weighted min-max game, their feature representations will fall into the feature space of  $\mathcal{D}_l \cup \mathcal{D}_{id}$ , so that they will act as ID data. Furthermore, they will be included in SSL training to improve the performance of our classification task on the interested classes.

### 2.3. Semi-supervised Learning

With the aforementioned OOD data detection and adversarial learning for recycling, we can take full advantage of class mismatched dataset by finding unlabeled ID data and recyclable OOD data, as well as filtering out the useless non-recyclable OOD data. Then, we can utilize the useful original labeled data, ID data and recyclable OOD data to implement semi-supervised learning by deploying any existing SSL regularizer to the  $\mathcal{L}_{ssl}$  in Eq. (1), such as consistency loss in [22, 24, 34], virtual adversarial training loss in [28], entropy minimization in [16], and so on.

Therefore, the general framework of the TOOR algorithm can be instantiated by substituting a specified SSL regularizer  $\mathcal{L}_{ssl}$  and the weighted min-max game in Eq. (6) into the ID data exploration term and OOD data recycling term in Eq. (1). Our TOOR method is summarized in Algorithm 1. Later experiments in Section 3.2 will show that TOOR can enhance many typical SSL methods in the class mismatch problem and achieve encouraging performance.

## 3. Experiments

In this section, we conduct exhaustive experiments to validate the proposed TOOR approach. Firstly, to show that our method is superior to traditional SSL methods in handling the class mismatch problem, we compare TOOR with popular SSL methods under different amounts of OOD data (Section 3.1). After that, we apply the TOOR framework to the aforementioned SSL methods and make comparisons with the state-of-the-art class-mismatched SSL methods (Section 3.2). Finally, detailed performance study will be provided to verify the effectiveness of the OOD data detection and recycling procedures in our TOOR approach (Section 3.3).

**Datasets.** In this paper, we use CIFAR-10 [21] and SVHN [29] datasets to evaluate the performance of our TOOR method. **CIFAR-10** contains 50,000 and 10,000 natural images with the size of  $32 \times 32$  for training and testing accordingly, which consist of six animal classes (e.g., “bird”, “cat”, “deer”, “dog”, “frog”, and “horse”) and four transportation tool classes (e.g., “airplane”, “automobile”, “ship”, and “truck”). Here we follow [17] by randomly choosing 2,400 images from the six animal classes to construct the labeled set, and picking up 20,000 images from all ten classes to compose the unlabeled set. By this way, the images belonging to the animal classes are ID data and those from the transportation tool classes are OOD data. **SVHN** is composed of 73,257 training images and 26,032 test images with the resolution of  $32 \times 32$ , which are collected from real-world house numbers. This dataset contains ten classes, namely the ten digits “0”~“9”. We randomly choose 600 images from the classes of “0”~“5” to compose the labeled set, and randomly sample 20,000 images from all ten classes “0”~“9” to form the unlabeled set.

**Implementation details of TOOR.** We adopt Wide ResNet-28-2 [41] as our backbone network, and send the output feature of *avg-pool* layer to the discriminator which has the same structure as in [6]. The flip-coefficient [12] of gradient reversal layer is gradually increased from 0 to 1. We train the network for 500,000 iterations with batch size of 100, and adopt Adam optimizer [20] with the initial learning rate  $3 \times 10^{-4}$ . Besides, the weight decay factor is set to 0.2 after 400,000 iterations. For the first 5,000 iterations, we only train the backbone network with supervised fidelity term to absorb enough label information which helps improve the performance of OOD data detection. Afterwards, we gradually ramp up the tradeoff parameter  $\lambda$  and  $\gamma$  using the same ramp up function as that in [30] to conduct SSL and adversarial domain adaptation.

### 3.1. Comparison with Traditional SSL Methods

To testify the capability of TOOR for class-mismatched SSL task, we vary the proportion of OOD data in the unlabeled set (denoted as  $\zeta$  hereinafter) to investigate the

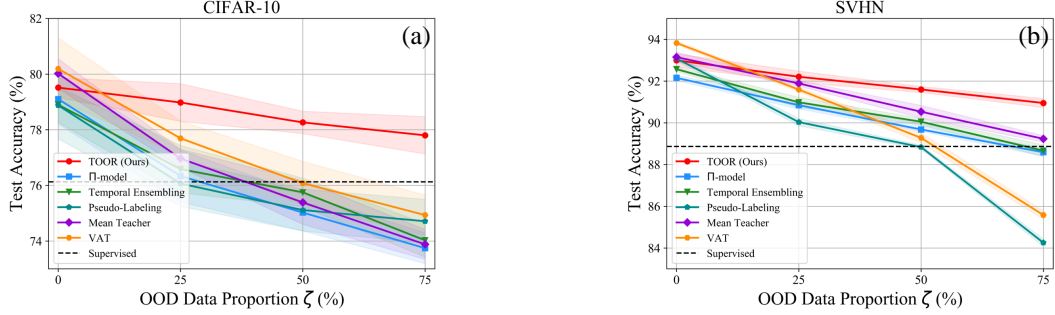


Figure 3. Experimental results of different SSL methods under class mismatch with varied  $\zeta$ . (a) Test accuracies on CIFAR-10 dataset. (b) Test accuracies on SVHN dataset. The shaded regions with the curves indicate the standard deviations of the accuracies of five runs.

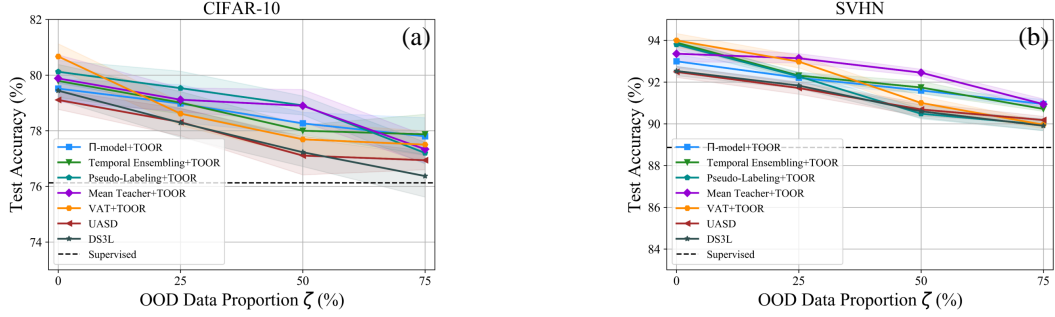


Figure 4. Experimental results of various methods in dealing with the class mismatch problem. (a) Test accuracies on CIFAR-10 dataset. (b) Test accuracies on SVHN dataset. The shaded regions with the curves indicate the standard deviations of the accuracies of five runs.

performances of various methods under different numbers of class-mismatched data. Concretely, we set  $\zeta$  to  $\{0\%, 25\%, 50\%, 75\%\}$  to observe the performances of TOOR and baseline methods, where  $\zeta = 0\%$  means that there are no OOD data. For TOOR, we adopt  $\Pi$ -model as the SSL regularizer  $\mathcal{L}_{ssl}$ , and the five traditional SSL methods for comparison include Pseudo-Labeling [24],  $\Pi$ -model [22, 32], Temporal Ensembling [22], VAT [28], and Mean Teacher [34]. Furthermore, we also train the backbone network Wide ResNet-28-2 on labeled set to form the ‘Supervised’ baseline. The detailed parameter settings of the baselines are provided in the supplementary material.

For both CIFAR-10 and SVHN, we randomly select OOD data for five times under each  $\zeta$  to establish the training set, and report the average test accuracies as well as the standard deviations of comparators over five independent runs. The experimental results on both datasets are shown in Figure 3. We can see that the performances of all baseline methods seriously degrade when  $\zeta$  increases, as the gradually incorporated OOD data significantly mislead the training of the above SSL approaches. In contrast, our method shows more stable performance than other SSL methods in both datasets, and constantly surpasses the supervised baseline, which demonstrates that TOOR successfully avoids the possible confusion brought by the OOD data in mismatched

classes. Specifically, when 75% unlabeled data are OOD data, our TOOR can still achieve 77.79% and 90.94% test accuracies on CIFAR-10 and SVHN, respectively, which are significantly higher than 74.93% and 89.23% achieved by the second best method.

### 3.2. Comparison with Class-Mismatched SSL Methods

In this part, we apply the TOOR framework to the traditional SSL methods including Pseudo-Labeling [24],  $\Pi$ -model [22, 32], Temporal Ensembling [22], VAT [28], and Mean Teacher [34], and compare them with two existing state-of-the-art approaches (*i.e.*, UASD [9] and DS<sup>3</sup>L [17]) that deal with class-mismatched SSL problem. Similar to Section 3.1, we also investigate the results of various methods under  $\zeta = \{0\%, 25\%, 50\%, 75\%\}$ , and the average accuracies of five runs on CIFAR-10 and SVHN datasets are shown in Figure 4. We can see that all the five traditional SSL methods combined with TOOR (*i.e.*, ‘ $\Pi$  model + TOOR’, ‘Temporal Ensembling + TOOR’, ‘Pseudo-Labeling + TOOR’, ‘Mean Teacher + TOOR’, and ‘VAT + TOOR’) perform satisfactorily, and the significant performance drop revealed by Figure 3 does not appear any more, which indicates that TOOR is quite general and can help many traditional SSL methods tackle the

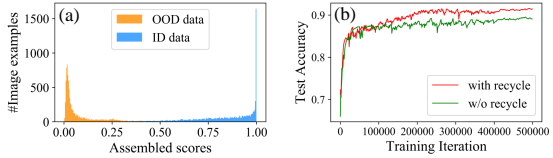


Figure 5. (a) Histogram of assembled softmax scores  $\hat{S}(\mathbf{x}; T)$  over all unlabeled images when supervised training finishes. (b) Test accuracies of different model configurations. Red curve: training with OOD data recycling. Green curve: training without recycling.

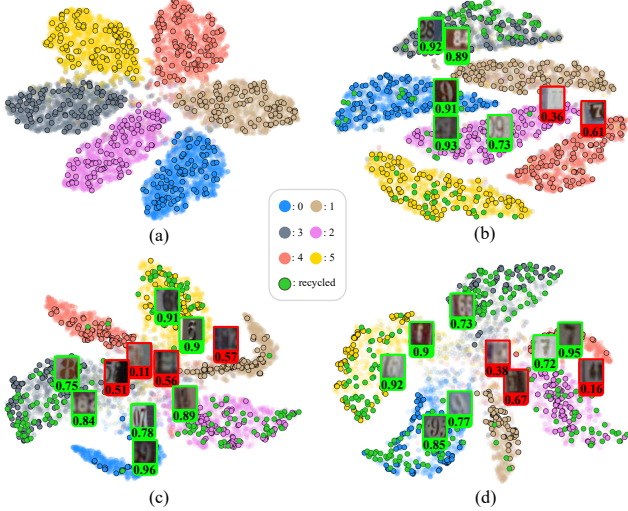


Figure 6. t-SNE visualizations of the image representations. Figures (a) ~ (d) correspond to the results obtained on SVHN with  $\zeta$  equaling 0, 0.25, 0.5, and 0.75, respectively. Different colors denote the image data from different classes, where the green dots indicate the recycled OOD data determined by TOOR, and the dots with black boundary denote the originally labeled data. Besides, some of the recyclable OOD images (green boxes) and non-recyclable OOD images (red boxes) are visualized, of which the transferability scores  $w(\mathbf{x})$  are also indicated below the images.

class mismatch problem. Moreover, the five SSL methods enhanced by TOOR outperform UASD and DS<sup>3</sup>L in most cases, which again demonstrates the effectiveness of our method. Specifically, when  $\zeta = 50\%$  which means half of the unlabeled images are OOD data, our “Mean teacher + TOOR” achieves the accuracy of 78.89%, which is much higher than UASD and DS3L with the accuracies 77.10% and 77.22% correspondingly on CIFAR-10 dataset. On SVHN dataset, the accuracy of “Mean teacher + TOOR” is as high as 92.45%, which outperforms UASD and DS3L with the accuracies 90.68% and 90.59% accordingly.

### 3.3. Performance Study

From the above experimental results presented in Sections 3.1 and 3.2, we can see that our TOOR achieves very encouraging results. Here we further analyze the effects of

key components in TOOR, and study the behind reasons for TOOR in achieving good performance. Specifically, we see that the OOD data detection in Section 2.1 and transferable OOD data recycling in Section 2.2 are critical to tackling class mismatch problem and boosting the performance, so next we validate their effectiveness, respectively. In the main paper, we only report the experimental results on SVHN dataset with  $\zeta = 0.5$ , and the results on CIFAR-10 dataset can be found in supplementary material.

**OOD data detection.** As mentioned in Section 2.1, The performance of OOD data detection largely depends on the computed assembled softmax scores in Eq. (4). To show the reasonability of our assembled softmax scores, we plot the scores of ID data and OOD data in Figure 5 (a). It is noteworthy that most of ID data have scores close to 1, and most of OOD data have scores close to 0. Therefore, the assembled softmax score provides valuable information in discriminating ID data and OOD data. As a result, in the experiment, we use a relatively large value 0.99 as the threshold  $\delta$  to guarantee that all decided ID data are correct, as the current excluded ID data are also possible to be recalled by the subsequent recycling procedure. However, if we use 0.5 as the threshold  $\delta$ , the erroneously incorporated non-recyclable OOD data will never have a chance to be discarded, which may further hurt the performance.

**OOD data recycling.** To further study the contributions of the recycling procedure, we compare the experimental results obtained by training our method with and without recycling. The results are shown in Figure 5 (b), which reveals that the recycling process is beneficial for our TOOR method to enhance the classification performance.

Furthermore, we provide the visualization of the image features extracted by Wide ResNet-28-2 via using t-SNE method [27] in Figure 6. It can be observed that most of the recycled OOD data (see the green dots) with relatively large transferability scores lie in the dense region within each cluster, while those with small transferability scores are distributed in a scattered way. Besides, we can see that the recycled OOD image data show great similarity to the classes in the labeled set. For example, we can see that many OOD data corresponding to digit “9” are mapped to the ID data with class “0”, as these two digits look similarly. In contrast, we can see that most of the non-recyclable OOD data in the red boxes are blurry and some of them cannot be recognized even by human. Hence, our method managed to alleviate the negative influence of these non-recyclable OOD data by assigning them with small transferability scores. In a word, our strategy of utilizing transferability to characterize recyclability makes sense, which is helpful to find the potential useful OOD data.

## 4. Conclusion

In this paper, we propose a novel SSL method termed TOOR that solves the class mismatch problem. Concretely, instead of completely discarding the detected OOD data, we adaptively weigh each OOD datum by quantifying their transferability to find the transferable OOD data, which can be further recycled via adversarial domain adaptation. As a result, the recycled OOD data can be re-used to help train a better semi-supervised classifier than existing methods. The comparison results with various SSL methods on benchmark datasets demonstrate the effectiveness of our proposed TOOR in handling class-mismatched datasets.

## References

[1] Mikhail Belkin, Partha Niyogi, and Vikas Sindhwani. Manifold regularization: A geometric framework for learning from labeled and unlabeled examples. *Journal of Machine Learning Research (JMLR)*, 7(Nov):2399–2434, 2006. 3

[2] Kristin P Bennett and Ayhan Demiriz. Semi-supervised support vector machines. In *NeurIPS*, pages 368–374, 1999. 2

[3] David Berthelot, Nicholas Carlini, Ian Goodfellow, Nicolas Papernot, Avital Oliver, and Colin A Raffel. Mixmatch: A holistic approach to semi-supervised learning. In *NeurIPS*, pages 5049–5059, 2019. 2

[4] Avrim Blum and Tom Mitchell. Combining labeled and unlabeled data with co-training. In *COLT*, pages 92–100, 1998. 2

[5] Zhangjie Cao, Lijia Ma, Mingsheng Long, and Jianmin Wang. Partial adversarial domain adaptation. In *ECCV*, pages 135–150, 2018. 2, 4

[6] Zhangjie Cao, Kaichao You, Mingsheng Long, Jianmin Wang, and Qiang Yang. Learning to transfer examples for partial domain adaptation. In *CVPR*, pages 2985–2994, 2019. 2, 4, 5, 6, 11

[7] Olivier Chapelle, Bernhard Scholkopf, and Alexander Zien. Semi-supervised learning. *IEEE Transactions on Neural Networks and Learning Systems (TNNLS)*, 20(3):542–542, 2009. 1

[8] Chaoqi Chen, Weiping Xie, Wenbing Huang, Yu Rong, Xinghao Ding, Yue Huang, Tingyang Xu, and Junzhou Huang. Progressive feature alignment for unsupervised domain adaptation. In *CVPR*, pages 627–636, 2019. 2

[9] Yanbei Chen, Xiatian Zhu, Wei Li, and Shaogang Gong. semi-supervised learning under class distribution mismatch. In *AAAI*, pages 3569–3576, 2020. 2, 7, 11, 14

[10] Zhihong Chen, Chao Chen, Zhaowei Cheng, Boyuan Jiang, Ke Fang, and Xinyu Jin. Selective transfer with reinforced transfer network for partial domain adaptation. In *CVPR*, pages 12706–12714, 2020. 2

[11] Yaroslav Ganin and Victor Lempitsky. Unsupervised domain adaptation by backpropagation. In *ICML*, pages 1180–1189. PMLR, 2015. 3, 11

[12] Yaroslav Ganin, Evgeniya Ustinova, Hana Ajakan, Pascal Germain, Hugo Larochelle, François Laviolette, Mario Marchand, and Victor Lempitsky. Domain-adversarial training of neural networks. *Journal of Machine Learning Research (JMLR)*, 17(1):2096–2030, 2016. 2, 4, 6

[13] Bo Geng, Dacheng Tao, Chao Xu, Linjun Yang, and Xian-Sheng Hua. Ensemble manifold regularization. *IEEE Transactions on Pattern Analysis and Machine Intelligence (TPAMI)*, 34(6):1227–1233, 2012. 3

[14] Chen Gong, Tongliang Liu, Dacheng Tao, Keren Fu, Enmei Tu, and Jie Yang. Deformed graph laplacian for semisupervised learning. *IEEE Transactions on Neural Networks and Learning Systems (TNNLS)*, 26(10):2261–2274, 2015. 1

[15] Ian Goodfellow, Jean Pouget-Abadie, Mehdi Mirza, Bing Xu, David Warde-Farley, Sherjil Ozair, Aaron Courville, and Yoshua Bengio. Generative adversarial nets. In *NeurIPS*, pages 2672–2680, 2014. 4

[16] Yves Grandvalet and Yoshua Bengio. Semi-supervised learning by entropy minimization. In *NeurIPS*, pages 529–536, 2005. 2, 6

[17] Lan-Zhe Guo, Zhen-Yu Zhang, Yuan Jiang, Yu-Feng Li, and Zhi-Hua Zhou. Safe deep semi-supervised learning for unseen-class unlabeled data. In *ICML*, 2020. 2, 6, 7, 11, 14

[18] Geoffrey Hinton, Oriol Vinyals, and Jeff Dean. Distilling the knowledge in a neural network. *arXiv preprint arXiv:1503.02531*, 2015. 4

[19] Ahmet Iscen, Giorgos Tolias, Yannis Avrithis, and Ondrej Chum. Label propagation for deep semi-supervised learning. In *CVPR*, pages 5070–5079, 2019. 2

[20] Diederik P Kingma and Jimmy Ba. Adam: A method for stochastic optimization. *arXiv preprint arXiv:1412.6980*, 2014. 6, 11

[21] Alex Krizhevsky, Geoffrey Hinton, et al. Learning multiple layers of features from tiny images. 2009. 6

[22] Samuli Laine and Timo Aila. Temporal ensembling for semi-supervised learning. In *ICLR*, 2016. 2, 3, 4, 6, 7, 11, 14

[23] Yann LeCun, Yoshua Bengio, and Geoffrey Hinton. Deep learning. *nature*, 521(7553):436–444, 2015. 2

[24] Dong-Hyun Lee. Pseudo-label: The simple and efficient semi-supervised learning method for deep neural networks. In *ICML Workshop*, volume 3, 2013. 2, 6, 7, 11, 14

[25] Shiyu Liang, Yixuan Li, and Rayadurgam Srikant. Enhancing the reliability of out-of-distribution image detection in neural networks. In *ICLR*, 2018. 4

[26] Yucen Luo, Jun Zhu, Mengxi Li, Yong Ren, and Bo Zhang. Smooth neighbors on teacher graphs for semi-supervised learning. In *CVPR*, pages 8896–8905, 2018. 2

[27] Laurens van der Maaten and Geoffrey Hinton. Visualizing data using t-sne. *Journal of Machine Learning Research (JMLR)*, 9(Nov):2579–2605, 2008. 8

[28] Takeru Miyato, Shin-ichi Maeda, Masanori Koyama, and Shin Ishii. Virtual adversarial training: a regularization method for supervised and semi-supervised learning. *IEEE Transactions on Pattern Analysis and Machine Intelligence (TPAMI)*, 41(8):1979–1993, 2018. 2, 6, 7, 11, 14

[29] Yuval Netzer, Tao Wang, Adam Coates, Alessandro Bissacco, Bo Wu, and Andrew Y Ng. Reading digits in natural images with unsupervised feature learning. In *NeurIPS Workshop*, 2011. 6

[30] Avital Oliver, Augustus Odena, Colin A Raffel, Ekin Dogus Cubuk, and Ian Goodfellow. Realistic evaluation of deep semi-supervised learning algorithms. In *NeurIPS*, pages 3235–3246, 2018. [2](#), [6](#), [11](#)

[31] Yingwei Pan, Ting Yao, Yehao Li, Yu Wang, Chong-Wah Ngo, and Tao Mei. Transferrable prototypical networks for unsupervised domain adaptation. In *CVPR*, pages 2239–2247, 2019. [2](#)

[32] Mehdi Sajjadi, Mehran Javanmardi, and Tolga Tasdizen. Regularization with stochastic transformations and perturbations for deep semi-supervised learning. In *NeurIPS*, pages 1163–1171, 2016. [7](#), [11](#), [14](#)

[33] Kihyuk Sohn, David Berthelot, Chun-Liang Li, Zizhao Zhang, Nicholas Carlini, Ekin D Cubuk, Alex Kurakin, Han Zhang, and Colin Raffel. Fixmatch: Simplifying semi-supervised learning with consistency and confidence. *arXiv preprint arXiv:2001.07685*, 2020. [2](#)

[34] Antti Tarvainen and Harri Valpola. Meanteachers are better role models: Weight-averaged consistency targets improve semi-supervised deep learning results. In *NeurIPS*, pages 1195–1204, 2017. [2](#), [3](#), [6](#), [7](#), [11](#), [14](#)

[35] Eric Tzeng, Judy Hoffman, Kate Saenko, and Trevor Darrell. Adversarial discriminative domain adaptation. In *CVPR*, pages 7167–7176, 2017. [2](#), [4](#)

[36] Fei Wang and Changshui Zhang. Label propagation through linear neighborhoods. *IEEE Transactions on Knowledge and Data Engineering (TKDE)*, 20(1):55–67, 2007. [1](#)

[37] Qin Wang, Wen Li, and Luc Van Gool. Semi-supervised learning by augmented distribution alignment. In *ICCV*, pages 1466–1475, 2019. [2](#)

[38] Yao Yao, Jiehui Deng, Xiuhua Chen, Chen Gong, Jianxin Wu, and Jian Yang. Deep discriminative CNN with temporal ensembling for ambiguously-labeled image classification. In *AAAI*, 2020. [5](#)

[39] Kaichao You, Mingsheng Long, Zhangjie Cao, Jianmin Wang, and Michael I. Jordan. Universal domain adaptation. In *CVPR*, 2020. [2](#)

[40] Bing Yu, Jingfeng Wu, Jinwen Ma, and Zhanxing Zhu. Tangent-normal adversarial regularization for semi-supervised learning. In *CVPR*, pages 10676–10684, 2019. [3](#)

[41] Sergey Zagoruyko and Nikos Komodakis. Wide residual networks. In *BMVC*, 2016. [6](#), [11](#)

[42] Xiaohua Zhai, Avital Oliver, Alexander Kolesnikov, and Lucas Beyer. S4l: Self-supervised semi-supervised learning. In *ICCV*, pages 1476–1485, 2019. [2](#)

[43] Jing Zhang, Zewei Ding, Wanqing Li, and Philip Ogunbona. Importance weighted adversarial nets for partial domain adaptation. In *CVPR*, 2018. [2](#), [4](#), [5](#)

[44] Liheng Zhang and Guo-Jun Qi. Wcp: Worst-case perturbations for semi-supervised deep learning. In *CVPR*, pages 3912–3921, 2020. [2](#)

[45] Dengyong Zhou, Olivier Bousquet, Thomas N Lal, Jason Weston, and Bernhard Schölkopf. Learning with local and global consistency. In *NeurIPS*, pages 321–328, 2004. [1](#)

## Supplementary Material

In the supplementary material, we first explain the implementation details of our TOOR and the baseline methods in Section A. Then we present the performance study results of our TOOR on CIFAR-10 dataset in Section B.

### A. Implementation Details

For all the investigated algorithms, we implement them by using the batch size of 100, and train each of them for 500,000 iterations. The network training for all methods is conducted by Adam optimizer [20] with the weight decay factor 0.2 after 400,000 iterations.

#### A.1. The Proposed TOOR

Here we present the experimental details of our TOOR by specifying the network architectures as well as the hyperparameter values.

**Backbone network  $F$ .** We choose the Wide ResNet-28-2 [41] as our backbone network  $F$ , and consider the last fully connected layer followed by a softmax operation as the classifier  $C$ . The architecture of the adopted Wide ResNet-28-2 is shown in Table 1. To achieve fair comparison, we implement all other methods by using the same backbone network as our TOOR method.

**Discriminator  $D$ .** We choose the same structure as in [6] to construct our discriminator, which is shown in Table 2. The flip-coefficient  $flip\_coeff$  in the GRL [11] aims to suppress the noisy signals from the discriminator at the early stages of training procedure, which ramps up from 0 to 1 by following the function  $flip\_coeff = \frac{2}{1+\exp(-10 \times (\text{iter} - \text{pretrain\_iter}) \times \frac{1}{400,000})} - 1$ , where  $\text{iter}$  denotes the current training iteration,  $\text{pretrain\_iter}$  denotes the number of iterations for supervised training and it is set to 5,000 in our experiments. The ramp up curve is shown in Figure 7 (a).

**Hyperparameters.** We set the temperature  $T$  in Eq. (2) of our main paper as 0.8 to compute the softmax scores, and set the OOD data detection threshold  $\delta$  as 0.99 for CIFAR-10 dataset and 0.999 for SVHN dataset to distinguish ID data from OOD data. The trade-off parameters  $\lambda$  and  $\gamma$  ramp up from 0 to 1 by following the functions  $\lambda = \exp(-5 \times (1 - \min(\frac{\text{iter}}{200,000}, 1))^2)$  and  $\gamma = \exp(-5 \times (1 - \min(\frac{\text{iter}}{400,000}, 1))^2)$ , respectively, which are shown in Figure 7 (b). Since our method is a general framework which can be applied to many traditional SSL methods, we use different initial learning rates for our backbone network by following the original settings of the adopted SSL methods. The detailed configurations are shown in Table 4. For discriminator  $D$ , we set the initial learning rate to 0.001.

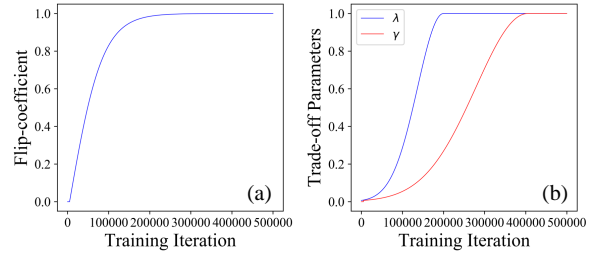


Figure 7. The ramp up curves of different parameters. (a) flip-coefficient  $flip\_coeff$ . (b) trade-off parameters  $\lambda$  and  $\gamma$ .

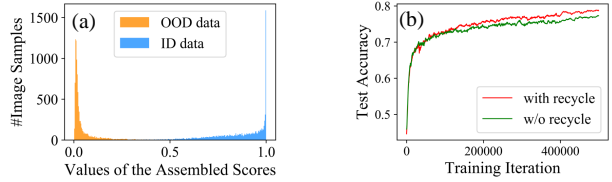


Figure 8. (a) Histogram of assembled softmax scores  $\hat{S}(\mathbf{x}; T)$  over all unlabeled images when supervised training finishes. (b) Test accuracies of different model configurations. Red curve: training with OOD data recycling. Green curve: training without recycling.

### A.2. Baseline Methods

For our compared baseline methods, we explain the details of the traditional SSL methods as well as the class-mismatched SSL methods.

**Traditional SSL methods.** For each traditional SSL method including Pseudo-Labeling [24],  $\Pi$ -model [22, 32], Temporal Ensembling [22], VAT [28], and Mean Teacher [34], we follow [30] and train the network by using different hyperparameter settings regarding the learning rate, decay schedule, and weight decay coefficients. The hyperparameter settings are summarized in Table 4.

**Class-mismatched SSL methods.** The compared class-mismatched SSL methods include UASD [9] and DS<sup>3</sup>L [17]. For UASD, we choose the ensemble size of the network predictions as 10, and set the OOD filter threshold as the average value of the confidence scores regarding all unlabeled data. For DS<sup>3</sup>L, we show the architecture of its weighting network in Table 3. Note that the meta network has the same architecture as its backbone network, which is shown in Table 1. The detailed hyperparameters of UASD and DS<sup>3</sup>L are also listed in Table 4.

## B. Performance Study on CIFAR-10 Dataset

In our main paper, we only provide the performance study results of our method on SVHN dataset. In this section, we follow the similar way as the main paper to conduct the performance study on CIFAR-10 dataset, which includes the investigations on the effectiveness of OOD data

Table 1. Architecture of backbone network  $F$ .

Group Name	Layer	Hyperparameters
	Input	$32 \times 32$ RGB image
	Translation	Randomly $\{\Delta x, \Delta y\} \sim [-2, 2]$
	Horizontal flip <sup>*</sup>	Randomly $p = 0.5$
	Gaussian noise	$\sigma = 0.15$
conv1	Convolutional	16 filters, conv $3 \times 3$
conv2	$\begin{bmatrix} \text{Batch-Normalization} \\ \text{Leaky-ReLU} \\ \text{Convolutional} \\ \text{Batch-Normalization} \\ \text{Leaky-ReLU} \\ \text{Convolutional} \end{bmatrix} \times 4$	$momentum = 1 \times 10^{-3}$ $negative\_slope = 0.1$ 32 filters, conv $3 \times 3$ $momentum = 1 \times 10^{-3}$ $negative\_slope = 0.1$ 32 filters, conv $3 \times 3$
conv3	$\begin{bmatrix} \text{Batch-Normalization} \\ \text{Leaky-ReLU} \\ \text{Convolutional} \\ \text{Batch-Normalization} \\ \text{Leaky-ReLU} \\ \text{Convolutional} \end{bmatrix} \times 4$	$momentum = 1 \times 10^{-3}$ $negative\_slope = 0.1$ 64 filters, conv $3 \times 3$ $momentum = 1 \times 10^{-3}$ $negative\_slope = 0.1$ 64 filters, conv $3 \times 3$
conv4	$\begin{bmatrix} \text{Batch-Normalization} \\ \text{Leaky-ReLU} \\ \text{Convolutional} \\ \text{Batch-Normalization} \\ \text{Leaky-ReLU} \\ \text{Convolutional} \end{bmatrix} \times 4$	$momentum = 1 \times 10^{-3}$ $negative\_slope = 0.1$ 128 filters, conv $3 \times 3$ $momentum = 1 \times 10^{-3}$ $negative\_slope = 0.1$ 128 filters, conv $3 \times 3$
avg-pool	Batch-Normalization Leaky-ReLU Average Pooling	$momentum = 1 \times 10^{-3}$ $negative\_slope = 0.1$ $outputszie = 1$
	Fully Connected	$classes = 6$
	Softmax	

<sup>\*</sup> Not applied on SVHN experiments.

Table 2. Architecture of our discriminator  $D$ .

Layer	Hyperparameters
GRL	flip-coefficient
Linear	$128 \rightarrow 1,024$
ReLU	
Dropout	$p = 0.5$
Linear	$1,024 \rightarrow 1,024$
ReLU	
Dropout	$p = 0.5$
Linear	$1,024 \rightarrow 1$
Sigmoid	

detection and OOD data recycling.

**OOD data detection.** To show the reasonability of the assembled softmax scores, we plot the scores of ID data and OOD data from CIFAR-10 dataset in Figure 8 (a). We can see the similar result as in the main paper, which indicates that our assembled score provides a valuable clue for separating ID data and OOD data.

Table 3. Architecture of the weighting network in DS<sup>3</sup>L.

Layer	Hyperparameters
Linear	$6 \rightarrow 100$
ReLU	
Linear	$100 \rightarrow 1$
Sigmoid	

**OOD data recycling.** We also conduct the similar experiments as in the main paper by comparing the performance obtained by training our method with and without recycling, which are shown in Figure 8 (b). We can see that the recycling procedure can promote the performance of our method in later stage of network training, which indicates that the recycling process is beneficial for our TOOR method to tackle the class mismatch problem.

Furthermore, we present the t-SNE visualization of image features from CIFAR-10 dataset in Figure 9. We can see that most of the recycled OOD data (see the green dots)

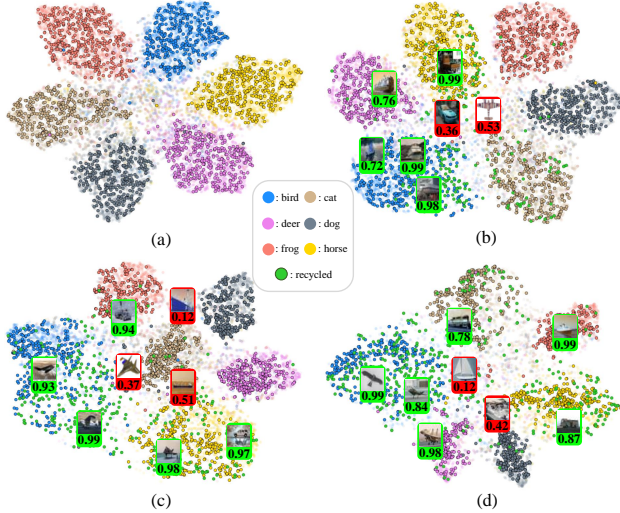


Figure 9. t-SNE visualizations of the image representations. Figures (a) ~ (d) correspond to the results obtained on CIFAR-10 dataset with OOD data proportion  $\zeta$  equaling 0, 0.25, 0.5, and 0.75, respectively. Different colors denote the image data from different classes, where the green dots indicate the recycled OOD data determined by TOOR, and the dots with black boundary denote the originally labeled data. Besides, some of the recyclable OOD images (green boxes) and non-recyclable OOD images (red boxes) are visualized, of which the transferability scores  $w(\mathbf{x})$  are also indicated below the images.

with relatively large transferability scores lie in the dense region within each cluster, while those with small transferability scores are distributed in a scattered way, which show the same results as in the main paper. Moreover, we can also see that the recycled OOD images show great similarity to the classes in the labeled set. For example, some of the “airplane” images are recycled to the “bird” classes, as they have similar shapes. On the other hand, some of the images show less similarity to the animal classes are assigned with small transferability scores, such as “0.12” and, “0.42”. To sum up, our strategy of utilizing transferability to characterize recyclability is still applicable in CIFAR-10 dataset and helps to exploit the potential information inherited by the OOD data in the mismatched classes.

Table 4. Hyperparameter settings of the compared SSL methods.

<b>Shared</b>	
learning rate decay factor	0.2
# training iteration in which learning rate decay starts	400,000
# training iteration in which consistency coefficient ramp up starts	200,000
<b>Supervised</b>	
Initial learning rate	0.003
<b>II-Model [22, 32]</b>	
Initial learning rate	$3 \times 10^{-4}$
Max consistency coefficient	20
<b>Temporal Ensembling [22]</b>	
Initial learning rate	$3 \times 10^{-4}$
Max consistency coefficient	20
Exponential moving average factor	0.6
<b>Mean Teacher [34]</b>	
Initial learning rate	$4 \times 10^{-4}$
Max consistency coefficient	8
Exponential moving average decay	0.95
<b>VAT [28]</b>	
Initial learning rate	0.003
Max consistency coefficient	0.3
$\epsilon$	6.0 or 1.0*
$\xi$	$10^{-6}$
<b>Pseudo-Labeling [24]</b>	
Initial learning rate	0.003
Max consistency coefficient	0.3
Pseudo-Labeling threshold	0.95
<b>UASD [9]</b>	
Initial learning rate	0.003
Ensemble size	10
<b>DS<sup>3</sup>L [17]</b>	
Initial learning rate for backbone network	0.003
Initial learning rate for meta network	0.001
Initial learning rate for weighting network	$6 \times 10^{-5}$

\* 6.0 for CIFAR-10 dataset and 1.0 for SVHN dataset.